ELSEVIER

Catalysis Today 33 (1997) 313–322

CATALYSIS TODAY

Molecular catalyst design. Synthesis, characterization and properties of zeolite NaY catalysts made with a tetranuclear copper(II) complex

Tarek M. Abdel-Fattah [a], Geoffrey Davies [b,*], Boris V. Romanovsky [c], Olga L. Shakhanovskaya [c], Alexei N. Larin [d], Susan A. Jansen [e], Michael J. Palmieri [e]

[a] *Chemistry Department, Michigan State University, East Lansing, MI 48824, USA*
[b] *Chemistry Department and the Barnett Institute, Northeastern University, Boston, MA 02115, USA*
[c] *Chemistry Department, Moscow State University, Moscow 117234, Russian Federation*
[d] *Chemistry Department, State Academy of Oil and Gas, Moscow 117296, Russian Federation*
[e] *Chemistry Department, Temple University, Philadelphia, PA 19122, USA*

Abstract

Highly active oxidation catalysts have been made by treating dehydrated zeolite NaY with excesses of the neutral tetranuclear copper(II) precursor $(\mu_4\text{-O})L_4Cu_4Cl_6$ (**A**, L = *N*,*N*-diethylnicotinamide) in methylene chloride, followed by methylene chloride washing, drying and oxidation with O_2 at 220°C. The loaded samples contain from 3.4 to 14.3% w/w total copper, depending on the amount of **A** used. Previous measurements with a different 'titration' loading method together with analytical and spectroscopic data for materials loaded with different excesses of **A** indicate 2.9–13.8% w/w copper on the zeolite surface (50 m^2/g) due to a zeolite–solution equilibrium with **A**. Oxidation of the most heavily loaded sample with O_2 gives a catalyst that is ten times more active per gram for CO oxidation than bulk CuO at 450°C. The most lightly loaded sample oxidizes CO 115 times faster than bulk CuO on a per gram CuO basis. Turnover numbers at infinitely dilute CuO loading approach 75% of the TON for bulk CuO, suggesting that CO oxidation on bulk CuO involves more than one CuO site. Prospects for catalyst development through transmetallation chemistry and different loading methods are discussed.

Keywords: Copper oxide; Zeolite; Carbon monoxide; Oxidation

1. Introduction

Supported metal or metal oxide cluster catalysts continue to attract strong interest. These catalysts emulate molecular species because of their uniformity. As a rule, they exhibit higher activity per unit mass than bulk materials because of their high dispersion [1–4].

Such catalysts are made by aqueous ion-exchange or by decomposing polymetallic precursors on the support surface under the mildest possible conditions. The aim is to avoid aggregation and agglomeration that give materials with bulk metal or metal oxide properties. This strategy requires loading the support with easily

* Corresponding author.

PII S0920-5861(96)00121-6

decomposed metal salts or polymetallic complexes.

Zeolites are useful industrial catalysts with high surface areas and different metal binding sites [5–8]. Ion-exchange of zeolites with aqueous solutions of salts like $NiCl_2$ gives Ni^{2+}–loaded materials. In principle, the loaded materials can be quantitatively reduced to highly dispersed, supported metal atoms or oxidized to give supported metal oxides. In practice, preference of cations like Ni^{2+} for inaccessible, high charge density intrazeolite sites makes high reduction temperatures necessary [9]. The result is metal aggregation and surface agglomeration that lessen the effectiveness of a zeolite support [9,10]. Controlling the distribution of mixed ions like Ni^{2+} and Cu^{2+} in a zeolite loaded by ion exchange is practically impossible, and incomplete conversion, aggregation and agglomeration problems remain on reduction to metals with H_2 or oxidation to metal oxides with O_2.

Use of families of structurally related, easily decomposed heteropolymetallic precursors offers the prospect of controlling supported mixed metal distribution in or on a support. An ability to study the effects of discrete metal substitution on activity would facilitate optimization and help to unravel catalytic mechanisms.

Tetranuclear copper(II) complexes $(\mu_4\text{-}O)L_4Cu_4Cl_6$ (where L is a monodentate amine) are easy to make and were first structurally characterized with L = pyridine [11]. The molecular structure of $(\mu_4\text{-}O)L_4Cu_4Cl_6$ (L = *N,N*-diethylnicotinamide) is shown in Fig. 1 [12]. This neutral complex contains a central oxo group tetrahedrally coordinated to four copper(II) centers. Each pair of copper(II) centers is bridged by chloride, resulting in trigonal $CuCl_3$ geometry at each copper. The central oxo group and the pyridine N of ligand L are co-linear with copper, resulting in approximate trigonal bipyramidal copper(II) coordination with the copper centers slightly displaced out of each $CuCl_3$ plane toward the pyridine N atom. The core dimensions of $(\mu_4\text{-}O)L_4Cu_4Cl_6$ (L = pyridine [11] or *N,N*-diethylnicotinamide [12])

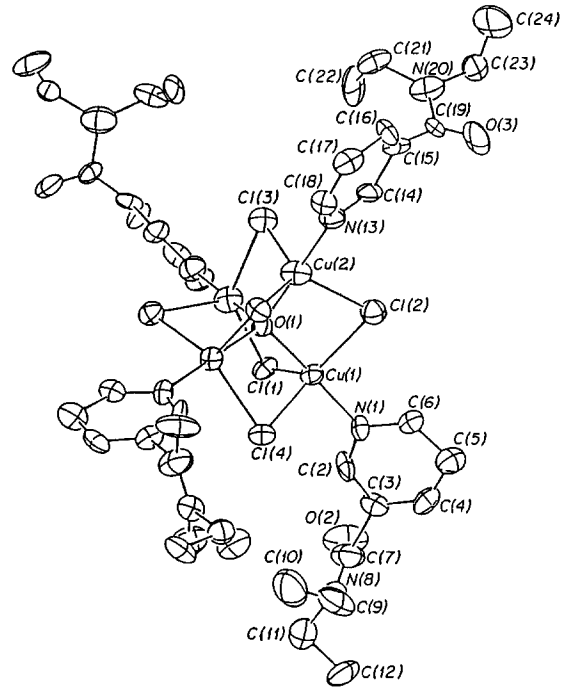

Fig. 1. Molecular structure of catalyst precursor $(\mu_4\text{-}O)L_4Cu_4Cl_6$, **A** (L = *N,N*-diethylnicotinamide [[12]]).

are virtually identical, but the latter complex is much more soluble in aprotic solvents like methylene chloride. High solubility recommended the use of $(\mu_4\text{-}O)L_4Cu_4Cl_6$ (L = *N,N*-diethylnicotinamide) as the precursor **A** for treatment of dehydrated zeolite NaY in this study.

Complex **A** has attractive properties as a catalyst precursor. Thermogravimetric measurements show that **A** rapidly loses its four *N,N*-diethylnicotinamide ligands L at 46 ± 1°C. The molecular core $(\mu_4\text{-}O)Cu_4Cl_6$ can then be stoichiometrically reduced to metallic copper with H_2 at 150°C (Eq. (1) [13–15]) or oxidized to copper(II) oxide with O_2 at 220°C (Eq. (2) [16]). Because of easy removal of L from **A**, the products are not contaminated with decomposed ligand fragments [13–16].

$$(\mu_4 - O)Cu_4Cl_6 + 4H_2 \rightarrow 4Cu + H_2O + 6HCl \quad (1)$$

$$(\mu_4 - O)Cu_4Cl_6 + 1.5O_2 \rightarrow 4CuO + 3Cl_2 \quad (2)$$

There are two ways of treating dehydrated zeolite NaY with precursor **A**.

The previously described 'titration' method [17] takes advantage of the intense brown color of **A** in aprotic solvents. Gradual addition of **A** to solid dehydrated NaY in anhydrous methylene chloride under N_2 at room temperature, with 30 min standing after each addition of **A** to ensure complete reaction, leads to the point where the supernatant is just visibly colored. This indicates a very slight excess of **A** in solution. The supernatant is removed and the loaded solid is washed with methylene chloride until the washings are clear and contain no ligand L released when the core $(\mu_4\text{-O})Cu_4Cl_6$ of precursor **A** enters the zeolite pore structure [17a,18]. Analysis of the loaded, washed and dried solid indicates that it contains 0.46% w/w Cu, with no copper on the zeolite surface or precursor ligand L in the sample [17]. The core $(\mu_4\text{-O})\text{–}Cu_4Cl_6$ of **A** is small enough (5.5 Å) to traverse the zeolite NaY pores (diameter 7.4 Å [6]) and is insoluble in methylene chloride [14]. The insolubility limits the amount of $(\mu_4\text{-O})\text{–}Cu_4Cl_6$ that can enter the zeolite pore structure. Three measurements supporting this conclusion are (1) there is no exchange of Na^+ in zeolite NaY by Cu^{2+} from **A** [17,18]; (2) the accessible surface area of the zeolite decreases from 740 to 50 m^2/gm as a result of copper loading by this method [17a,18]; and (3) the loaded product is essentially impervious to water, whereas dehydrated zeolite NaY absorbs 24% w/w water on standing in air [17a,18].

These data indicate that the precursor core $(\mu_4\text{-O})Cu_4Cl_6$ blocks the interior of zeolite NaY and that only about 7% of the total zeolite surface area is exterior (cf. [6]). Use of the 'titration' loading method in refluxing methylene chloride at 40°C gives the same copper loading and loaded sample properties [17a,18].

A second 'excess' loading method treats dehydrated zeolite NaY with large excesses of precursor **A** in refluxing methylene chloride. As will be seen, the loaded zeolite now contains from 3.4 to 14.3% w/w total copper, depending on the amount of precursor **A** used in the experiment. Based on the previous measurements [17], no more than 0.46% of copper is incorporated in the zeolite pore structure by this method. That is, from 2.9 to 13.8% w/w copper is on the zeolite outer surface (area 50 m^2/gm [17a]).

This paper describes the characterization of catalysts made by the 'excess' loading method. Thorough washing of the loaded samples to remove excess **A** and ligand L was followed by drying and oxidation of the loaded samples with O_2 at 220°C. Data for the oxidized products indicate highly dispersed copper(II) oxide that catalyzes CO oxidation much more efficiently than bulk CuO. The catalysts are reversibly converted to carbonatocopper(II) species on exposure to ambient air.

2. Experimental

2.1. Materials

Methylene chloride was purified by washing with (1) concentrated H_2SO_4 and (2) water and was then stored over calcined 5A molecular sieves. Precursor $(\mu_4\text{-O})L_4Cu_4Cl_6$ (**A**, Fig. 1) was synthesized and crystallized as before [12].

Zeolite NaY (Strem, 1 μm) was pelleted with no binder and calcined at 550°C for 6 h. The calcined pellets were carefully crushed and fractionated into 0.5–1.0 mm particles. The 3 g fractionated sample used for all experiments was heated under vacuum at 450°C for 6 h. After cooling under vacuum to room temperature, it was transferred to a glove box purged overnight with dry N_2 and divided into three 1 g portions. The first portion was treated overnight with 1.33 mmol of precursor **A** in refluxing, purified methylene chloride. The loaded solid was isolated and repeatedly washed with purified methylene chloride until the washings contained no **A** or ligand L. The washed solid was dried under vacuum at 60°C overnight and was then treated with flowing O_2 at 220°C for 10 h [16]. The other 1 g zeolite samples were treated

respectively with 0.66 and 0.33 mmol of **A** in the same volume of methylene chloride with the same procedure.

2.2. Analytical methods

The copper contents of the loaded zeolite samples were measured by digesting a known weight of sample in H_2SO_4/HNO_3 and spectrophotometric measurement with pyridineazoresorcinol, as described previously [19]. The results were checked by atomic absorption spectroscopy of the acid digests with a Buck model 200A instrument calibrated with certified copper standards. The data were corrected for matrix effects by measurements with unloaded zeolite NaY.

Infra red spectra of solid zeolite NaY and loaded, oxidized samples that had been exposed to ambient air were obtained in KBr disks with a Nicolet IR142 instrument. X-ray diffractograms of solid zeolite NaY and ambient air-exposed loaded, oxidized samples were measured with a Rikagu Rotaflex instrument with a rotating anode and Cu K_α radiation (λ = 0.15418 Å). EPR spectra of loaded, oxidized samples were measured from 25 to 450°C with a Bruker ER200 X-band spectrometer. This instrument is fitted with a Bruker ER035 gaussmeter with a minimum resolution of 0.1 G at a scan rate of 0.25 G/s and with a Bruker ER201 frequency controller. Spectra were collected through an interfaced 486 MHz personal computer and simulated with theory based on a second-order perturbation effect [20]. The sample temperatures were varied and controlled to $\pm$0.5 K with a Bruker ER4114 device.

The oxygen storage capacities of the loaded samples were determined with a pulse technique. About 100 mg of sample was loaded into a quartz reactor (3 mm i.d.) and heated at 450°C for 2 h in dry, flowing N_2 (30 ml/min). Eight to ten pulses of pure CO (1 ml) were introduced into the carrier gas and the CO_2 produced was quantitatively determined by gas chromatography. Blank experiments with unloaded zeolite NaY gave no CO oxidation. A conventional bulk CuO catalyst was made by treating aqueous $Cu(NO_3)_2$ solution with ammonia. The precipitated $Cu(OH)_2$ was washed with water, dried and calcined in air at 800°C for 10 h. The surface area of the CuO product (8.6 m^2/gm) was measured by the standard BET method at 77 K with N_2.

2.3. Catalytic measurements

Catalysis of CO oxidation to CO_2 by O_2 was investigated in a gradientless glass reactor at 450°C and 1 atm. The thoroughly dried feedstock had molar ratio $CO/O_2 = 1.0$. Production of CO_2 was monitored by gas chromatography.

3. Results and discussion

3.1. Elemental analysis

Elemental analyses (Table 1) of the catalysts prepared as described above show that the loading of fractionated, dehydrated zeolite NaY with copper depends on the amount of precursor **A** in the methylene chloride treatment solution. As explained earlier, the intrazeolite capacity of dehydrated NaY for the core $(\mu_4\text{-O})Cu_4Cl_6$ of precursor **A** is 0.46% w/w copper [17,18]. The data in column 3 of Table 1 thus refer to the weight percentage of copper on the zeolite surface, with surface area 50 m^2/g [17a]. Thus, the percentage of total copper on the surface of the samples labelled in Table 1 is $2.9/3.4 \times 100 =$ 85, 95 and 97, respectively.

It is important to emphasize that loading of dehydrated zeolite NaY with precursor **A** by the

Table 1
Copper oxide contents of loaded and oxidized zeolite NaY

Designation	CuO (% w/w)	Surface CuO (% w/w) [a]
3CuO/NaY	3.4	2.9
9CuO/NaY	9.4	8.9
14CuO/NaY	14.3	13.8

[a] See text for estimation method.

'titration' method is stoichiometric and limited by the solubility of its core $(\mu_4\text{-O})Cu_4Cl_6$ in methylene chloride [14,17,18]. However, zeolite surface loading with copper from excess **A** in methylene chloride is an equilibrium process, as indicated by the following. Sample 3CuO/NaY (Table 1) was made by zeolite treatment with 0.33 mmol **A**. Stoichiometric reaction would give 8.5% w/w copper loading, with 8.0% w/w on the surface, but the result is 2.9% (Table 1, row 1, column 3). Thus, 5.1/8.5 = 60% of **A** remains in the brown treatment solution, and is washed away with methylene chloride. Similar consideration of the result of treating zeolite NaY with 0.66 and 1.33 mmol of **A** in the same volume of methylene chloride indicates that about half of the total **A** is not adsorbed (the treatment solutions are brown, as before). Thus, while zeolite NaY encapsulation of cores $(\mu_4\text{-O})\text{–}Cu_4Cl_6$ from **A** is stoichiometric, reaction of **A** with the zeolite surface is an equilibrium that involves exchange of precursor ligands L with surface zeolite donor atoms. This is reasonable because the number and geometry of intrazeolite and surface donor atoms are quite different [6].

It follows that most of the properties of the loaded, oxidized materials described in the following sections refer to surface copper(II) species. The oxidized samples contained negligible chlorine, indicating no incorporation of chlorine from Cl_2 generated in reaction (2).

3.2. X-ray diffraction

Fig. 2 shows the X-ray diffractogram of sample 9CuO/NaY (Table 1) after loading, oxidation with O_2 at 220°C, catalytic use for CO oxidation at 450°C for 3 h and exposure to ambient air. This protocol leaves crystalline zeolite NaY with unchanged diffraction peaks along with additional peaks (*) due to copper species. These additional peaks are indexed in Table 2. Comparison with literature lattice pa-

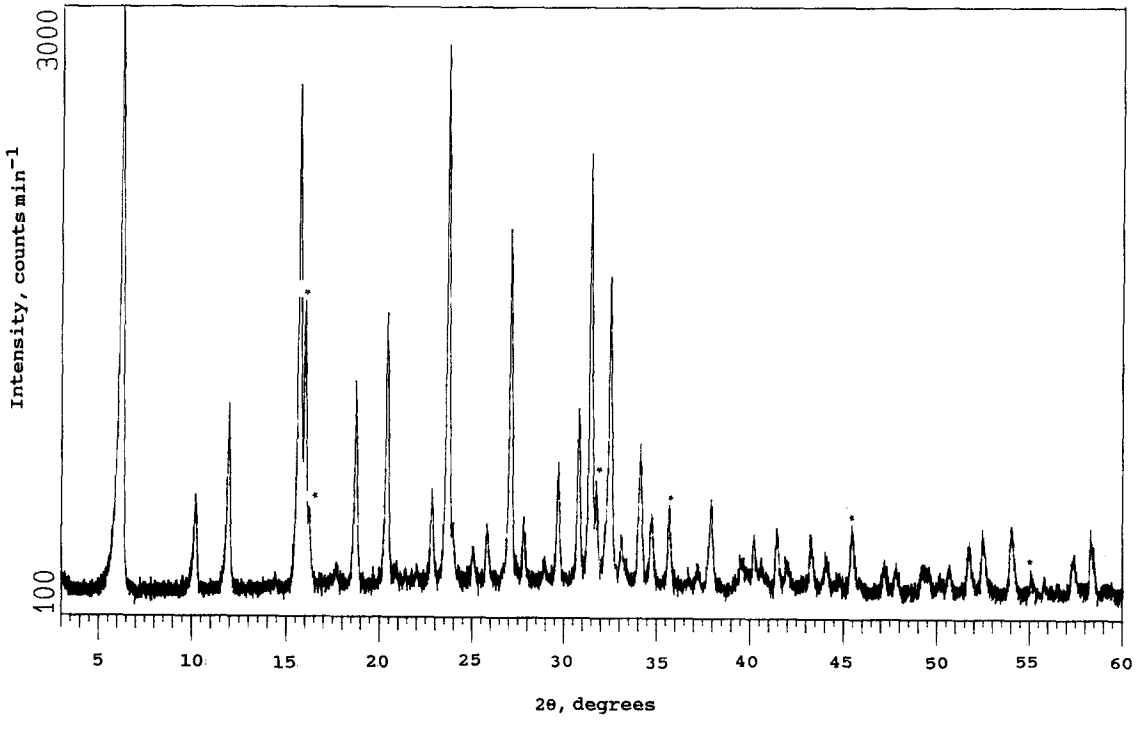

Fig. 2. X-ray diffractogram of oxidized, ambient air-exposed zeolite sample 9CuO/NaY. Peaks not observed in unloaded zeolite NaY are indicated '*'.

rameters (Å) and relative peak intensities for known copper carbonates [21] suggests that the additional peaks are due to the presence of $Na_2Cu(CO_3)_2 \cdot 3H_2O$ (Table 2), although the peak with $d = 5.512$ Å has a larger relative intensity than expected for this compound [21]. Thus, there probably is more than one copper(II) species on the surface of the ambient air-exposed, loaded and oxidized zeolite (see below).

It is important to note that loading of dehydrated zeolite NaY with precursor **A** by the 'titration' loading method (see Introduction [17,18]), washing with methylene chloride, drying and oxidation with O_2 at 220°C gives products that have little tendency to react with CO_2 in ambient air [18]. Thus, the '*' peaks in Fig. 2 are due to formation of surface carbonatocopper(II) products with close to the weight percentage in row 2, column 3 of Table 1.

3.3. FTIR spectra

The formation of carbonatocopper(II) products on exposure of loaded, washed, dried and oxidized zeolite sample 9CuO/NaY to ambient air is supported by additional features in the FTIR spectrum of zeolite NaY due this protocol (Fig. 3). The doublet near 860 cm^{-1} and the singlet at 680 cm^{-1} are characteristic of carbonato species [22,23]. Strong zeolite absorption at other frequencies characteristic of carbonatocopper(II) compounds [22] makes assignment difficult, but the two features in Fig. 3 do not rule out the presence of $Na_2Cu(CO_3)_2 \cdot 3H_2O$ suggested by the data in Fig. 2 and Table 2.

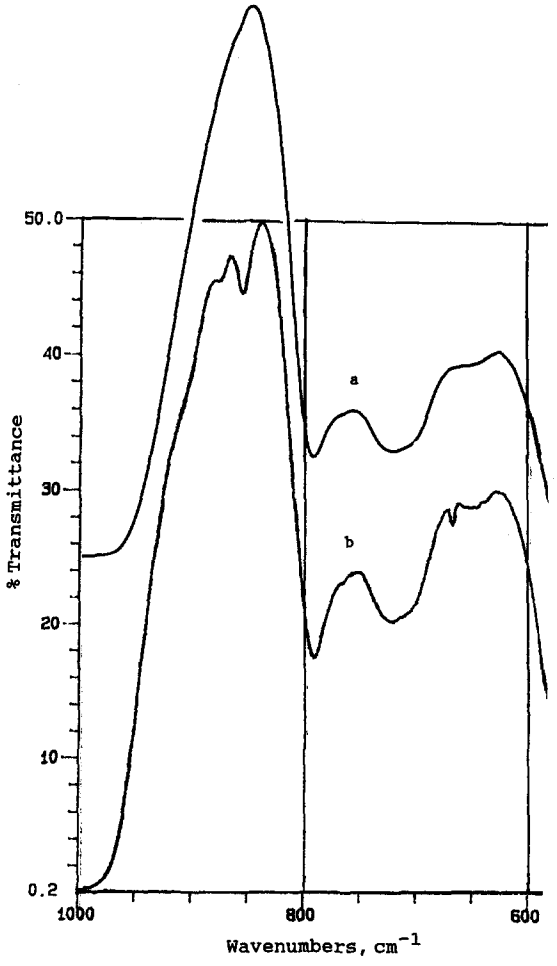

Fig. 3. FTIR KBr disk spectra of (a) zeolite NaY and (b) oxidized sample 9CuO/NaY in ambient air.

Table 2
Lattice parameters (Å) from X-ray diffraction data [a]

9CuO/NaY	$Na_2Cu(CO_3)_2 \cdot 3H_2O$
1.665(1)	[b]
1.994(5)	1.999(5)
2.514(4)	2.600(3)
2.822(5)	2.89(6)
5.482(5)	5.59(4) [c]
5.512(25)	[b]

[a] Numbers in parentheses are relative intensities of the '*' peaks in Fig. 2.
[b] Not reported in [[21]].
[c] See comments in text.

3.4. EPR spectra

The room temperature EPR spectrum of loaded, washed, dried, oxidized and ambient air-exposed zeolite sample 9CuO/NaY (Fig. 4) is well simulated by a single orthorhombic carbonatocopper(II) species with the parameters in Table 3. The spectrum and simulation indicate hyperfine coupling of less than 106 MHz (30 G), which is less than the spectral linewidth and thus is unresolved. Fig. 5 shows the effect of heating this sample in O_2 for 6 h at 120°C. The

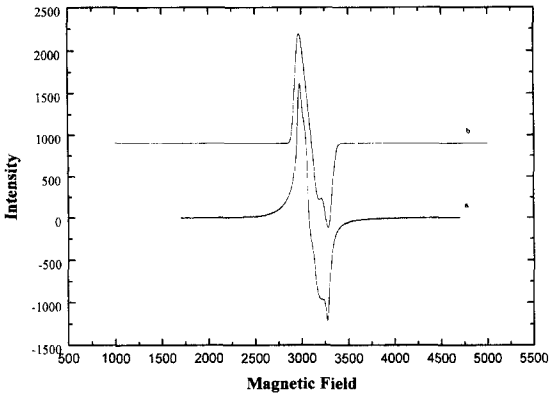

Fig. 4. (a) Observed and (b) simulated EPR spectra of oxidized sample 9CuO/NaY at room temperature in ambient air. Calculated parameters [20] are given in Table 3.

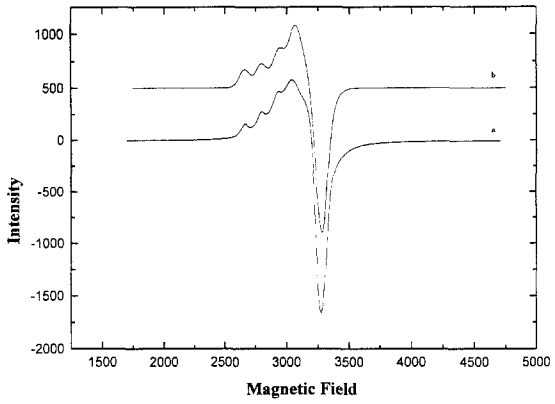

Fig. 5. Observed (a) and simulated (b) EPR spectra of the product of heating the sample in Fig. 4 at 120°C in O_2 for 6 h. Calculated parameters [20] are given in Table 3.

spectrum is well simulated by a single axial CuO species with parameters in Table 3 that resemble those for CuO on different alumina and silica surfaces. Heating this sample at 300°C and then 450°C has very little effect on its axial EPR spectrum (Fig. 6, Table 3). It is important that the average g value $< g >_{av}$ remains essentially the same throughout this heating protocol and that there is no significant change in spin concentration on heating the sample. These results indicate no CuO migration or agglomeration to form diamagnetic CuO domains on sample heating to at least 450°C, the temperature used for catalytic measurements.

The sample heated at 450°C was exposed with agitation to a slight positive pressure of dry CO_2 for 18 h at room temperature and then stored in ambient air for 1 h. Its room temperature EPR spectrum was measured after this treatment. Fig. 7 indicates that the reaction of surface CuO with CO_2 is reversible. Quantitative spectral subtraction revealed that the products of this sample protocol are 70% of the original carbonatocopper(II) species (Fig. 4), 10–15% of the unreacted CuO product of heating at 450°C (Fig. 6), and 5–15% of a third unidentified paramagnetic copper(II) species. The spectra in Fig. 7 become more similar on longer exposure to ambient air. This is strong evidence for reactive, highly dispersed CuO on the zeolite catalyst surface.

It is important to note that loading of dehydrated zeolite NaY with precursor **A** by the 'titration' method, washing with methylene chloride, drying and oxidation with O_2 at 220°C gives EPR-silent products. This indicates even numbers of electronically coupled CuO units

Table 3
EPR parameters for oxidized sample 9CuO/NaY [a]

	g_1	g_2	g_3	$< g >_{av}$	$A_{\|}$ (MHz)
In ambient air, then	2.3416	2.2380	2.1186	2.2327	[b]
Heated to 120°C, then	2.3489	2.1264	2.0786	2.1846	450
Heated to 450°C	2.4086	2.0887	2.0887	2.1953	410

[a] See Figs. 4–7 and text for discussion of data.
[b] Not resolved (see text).

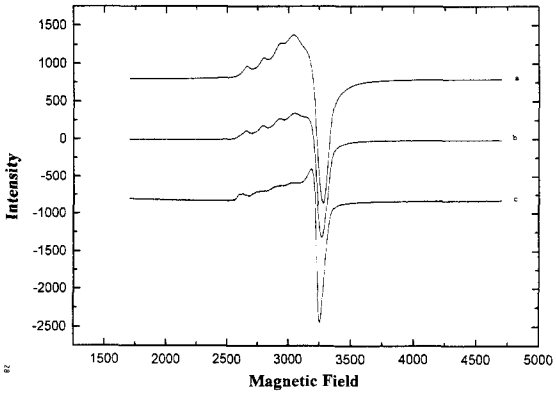

Fig. 6. Observed EPR spectra for sample 9CuO/NaY in O_2 at (a) 120°C, (b) 300°C and (c) 450°C. Calculated parameters [20] are given in Table 3.

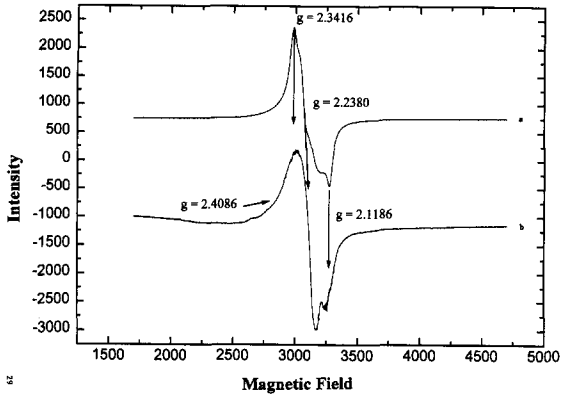

Fig. 7. Room temperature EPR spectra of air-exposed, oxidized sample 9CuO/NaY (a) and the result (b) of (1) heating this sample at 450°C, (2) room temperature reaction with dry CO_2, and (3) exposure of the product from (2) to ambient air. See text for discussion.

(bulk CuO is diamagnetic). The simplest explanation for EPR silence is the presence of Cu_4O_4 units in the supercavity (diameter 13.4 Å [6]) of zeolite NaY, with no migration of odd units of CuO to other zeolite Y locations (hexagonal channel, sodalite cage [6,23,24]) on sample heating to at least 250°C [16,17].

EPR activity in Figs. 4–7 indicates odd numbers of paramagnetic, surface copper(II) species. Assuming we have zeolite-anchored, single CuO units from surface reaction (1), the area occupied by each surface CuO unit in the samples (Table 1, column 3) is 19, 5.9 and 3.8 $Å^2$/CuO unit, respectively. If we approximate each area as a square, the respective edge lengths are 4.3, 2.4 and 2.0 Å. The estimates for samples 9CuO/NaY and 14CuO/NaY are close to the Cu–O distance 1.97 Å in bulk CuO [24], and would predict significant pairwise OCu–CuO coupling and EPR silence (but see Figs. 4–7). Anchoring of surface CuO units by coordination to $(HO,O)_m(Si,Al)_n$ zeolite sites prevents CuO migration to give diamagnetic bulk copper(II) oxide up to temperatures of at least 450°C (Fig. 6). Simple geometric estimation with known Si–O–Si(Al) distances and angles [6] predicts that having CuO units normal to the zeolite surface separates them sufficiently to prevent significant OCu–CuO coupling even in the most heavily loaded sample 14CuO/NaY in Table 1.

3.5. Oxygen storage capacity

Table 4 lists the oxygen storage capacities (OSC) measured by high temperature reaction of the samples with CO and their total copper contents (TCC, Table 1, column 2) from elemental analysis. As seen, the OSCs per gram of zeolite are similar to that for bulk CuO even though they contain ten times less copper. Thus, almost all the oxygen atoms of the copper-zeolite catalysts react with CO. In other words, the reactivity of zeolite-supported CuO is ten times higher than that of bulk CuO. This difference is attributed to uniform, high dispersion of the active component, as indicated in the previous sections.

3.6. Catalytic activity

The data for catalyzed CO oxidation by O_2 in Table 5 support the conclusion from OSC data. The rate of CO oxidation per gram CuO of the zeolite-supported catalysts is 70–115 times higher than for bulk CuO. Good agreement with the OSC values in Table 4 is further evidence for highly dispersed CuO in this catalyst system.

Different turnover numbers are expected for CuO units in different geometrical and electronic environments [24]. The TON of the most heavily loaded sample 14CuO/NaY (97% sur-

Table 4
Oxygen storage capacities of CuO-NaY samples

Sample	OSC (mmol O/g) [a]	TCC (mmol Cu/g) [b]	Ratio Cu/O
3CuO/NaY	0.40	0.42	1.05
9CuO/NaY	1.04	1.19	1.14
14CuO/NaY	1.53	1.86	1.22
CuO	1.04	12.6 [c]	12.1

[a] OSC = oxygen storage capacity.
[b] TCC = total copper content.
[c] Calculated for bulk CuO.

face CuO) is 2.5 times less than for bulk CuO. However, we saw earlier that the CuO unit separation distances approach that in bulk CuO with increasing zeolite loading. Also, the TON in Table 5 increase with decreasing copper oxide content and approach $(2.05 \pm 0.05) \times 10^2$ CO molecules/s Cu atom at infinite dilution on zeolite NaY. This is 75% of the TON for bulk CuO under the same conditions (Table 5). It appears that CO oxidation on bulk CuO has cooperative character and involves more than one copper site [24].

3.7. Prospects for catalyst development

Complex $(\mu_4\text{-O})L_4Cu_4Cl_6$ is readily transmetallated (Eq. (3) [12,25,26]). Here, x is 1, 2, 3 or 4 and NS is a monoanionic hydrazinedithiocarboate ligand in transmetallators $M(NS)_n$. Reactions (3) are rapid and stoichiometric in ambient aprotic solvents and the products are easily separated [25]. Variation of M = Co, Ni or Zn at each stoichiometric step theoretically gives a structurally

$$(\mu_4\text{-O})L_4Cu_4Cl_6 + xM(NS)_2 \rightarrow (\mu_4\text{-O})L_4Cu_{4-x}M_xCl_6 + xCu(NS)_2 \quad (3)$$

similar family of 36 different tetranuclear molecules. An example is $(\mu_4\text{-O})L_4CoNiCuZnCl_6$, which contains four different metals [26].

Transmetallation targets and heteropolymetallic transmetallation products are easily decomposed, first by low temperature loss of ligands L (see above [13]) and then to the corresponding metals (with H_2 in the analogue of Eq. (1) [13,14] or spontaneously with no external reductant [15]) or to metal oxides (with O_2 in the analogue of Eq. (2) [16]). For example, reduction of the family $(\mu_4\text{-O})L_4Cu_{4-x}Ni_xCl_6$ (x = 1, 2, 3 or 4) with H_2 gives the corresponding single phase alloys when $x = 1$, 2 or 3 and highly dispersed metallic nickel when $x = 4$ [13–15]. Oxidation with O_2 gives the respective pure or mixed metal oxides at 220–250°C. An example is conversion of $(\mu_4\text{-O})L_4Cu_2Ni_2Cl_6$ to uniform, highly dispersed equimolar CuO and NiO [16].

Use of the 'titration' zeolite loading method gives products with the same molar ratios of metals as in the heteropolymetallic precursors used to make them [17,18]. The 'excess' precursor loading method of the present work would put additional metal on the zeolite surface.

Treatment [17] of dehydrated zeolite NaY with ambient aprotic solutions of precursors $(\mu_4\text{-O})L_4Cu_{4-x}Ni_xCl_6$ (L = *N*,*N*-diethylnicotinamide, $x = 0$, 1, 2, 3 or 4) by the 'titration' method [17] results in loss of L and encapsulation of their respective cores $(\mu_4\text{-O})Cu_{4-x}Ni_xCl_6$ in zeolite NaY, as indicated by the following evidence [18].

Ligand L has a strong IR band at 1635 cm^{-1} that is absent in the loaded, washed and dried zeolite samples, which contain negligible carbon. X-ray photoelectron spectra of the samples before and after oxidation (with O_2 at 220°C) or reduction (with H_2 up to 350°C) indicate negligible surface copper or nickel species. The EPR spectra of $(\mu_4\text{-O})L_4Cu_{4-x}Ni_xCl_6$ are rhombic,

Table 5
Activity of zeolite NaY-supported and bulk copper oxide in CO oxidation at 450°C

	3CuO/NaY	9CuO/NaY	14CuO/NaY	CuO [a]
Reaction rate (mmol/s)				
Per gram of catalyst	0.75×10^2	1.84×10^2	2.01×10^2	1.94×10^1
Per gram of CuO	2.23×10^3	1.95×10^3	1.36×10^3	1.94×10^1
Turnover number molecule/s Cu atom	1.78×10^2	1.55×10^2	1.08×10^2	2.71×10^2

[a] Calculations for CuO based on a surface concentration of 5×10^{18} atom/m^2 and a surface area of 8.6 m^2/gm (see text).

as expected for trigonal bipyramidal copper(II) centers (Fig. 1). In contrast, dehydrated zeolite NaY samples loaded by 'titration' with $(\mu_4\text{-O})L_4Cu_{4-x}Ni_xCl_6$ ($x = 1$, 2 or 3) all have axial EPR spectra with closely similar parameters, consistent with loss of ligand L on zeolite loading and lower than trigonal pyramidal copper(II) symmetry in the products. An example is encapsulation of $(\mu_4\text{-O})Cu_2Ni_2Cl_6$, which results in the characteristic axial copper(II) EPR spectrum. Precursors $(\mu_4\text{-O})L_4Cu_{4-x}Ni_xCl_6$ are all too large (diameter $\simeq 17$ Å [18]) to fit the zeolite NaY pores ($\simeq 7.4$ Å [6]) but they can exchange their L ligands for intrazeolite atoms (presumably Al, Si–*O*H or Al, Si–O^-) of the zeolite, as shown for other encapsulated tetrametallic species [27].

We recommend the use of easily decomposed polynuclear transmetallation targets and heteropolynuclear transmetallation products as precursors to make metallated zeolites with designed and controlled atomic ratios of different metals. The 'titration' loading method apparently gives exclusive intrazeolite products, while the 'excess' precursor loading method puts additional metal species on the zeolite surface. We are exploring heteropolymetallic catalysts made from heteropolymetallic transmetallation products along with different loading methods. The results will distinguish intrazeolite and surface processes and delineate the effects of controlled metal substitution on catalysis. This will help the design of effective catalysts like those based on copper chemistry for oxidation of CO [28], the main toxic flue gas.

Acknowledgements

We gratefully acknowledge financial support from the Petroleum Research Fund, administered by the American Chemical Society, and the Russian Foundation for Fundamental Researches. This is contribution number 639 from the Barnett Institute at Northeastern University.

References

[1] Y. Wang and N. Herron, J. Phys. Chem., 91 (1987) 257.
[2] G. Schulz-Eckloff, Stud. Surf. Sci. Catal., 69 (1991) 65.
[3] G. Larsen and G.L. Haller, Catal. Today, 15 (1992) 431.
[4] R.J. Davis, Heterog. Chem. Rev., 1 (1994) 41.
[5] J.M. Thomas, Sci. Am., 266 (1992) 112
[6] J.M. Thomas and C.R.A. Catlow, Progr. Inorg. Chem., 35 (1987) 1.
[7] G.T. Kerr, Sci. Am., 261 (1989) 100.
[8] C.T. Kresge, M. Leonowicz, W. Roth, J. Vartuli and J. Beck, Nature, 359 (1992) 710.
[9] B. Coughlan and M.A. Keane, J. Catal., 123 (1990) 364; J. Catal., 136 (1992) 170; Can. J. Chem., 68 (1990) 1471; Zeolites, 11 (1991) 2.
[10] P.B. Malia, P. Ravindranathan, S. Komarneni, E. Breval and R. Roy, Mater. Res. Soc. Symp. Proc., 233 (1991) 207.
[11] B.T. Kilbourne and J.D. Dunitz, Inorg. Chim Acta, 1 (1967) 209.
[12] A. El-Toukhy, C.-Z. Cai, G. Davies, T.R. Gilbert, K.D. Onan and M. Veidis, J. Am. Chem. Soc., 106 (1984) 4596.
[13] J.V. Marzik, L.G. Carriera and G. Davies, J. Mater. Sci. Lett., 7 (1988) 833; US Pat., 4 933 003 (1990).
[14] G. Davies, B.C. Giessen and H.-L. Shao, Mater. Lett., 9 (1990) 231
[15] G. Davies and H.-L. Shao, US Pat., 5 061 313 (1991).
[16] G. Davies, B.C. Giessen and H.-L. Shao, Mater. Res. Soc. Symp. Proc., 249 (1992) 87.
[17] (a) T.M. Abdel-Fattah, Doctoral Dissertation, Northeastern University, 1994; (b) T.M. Abdel-Fattah and G. Davies, in C.A.C. Sequiera and M.J. Hudson, Editors, Multifunctional Mesoporous Inorganic Solids, Kluwer, Dordrecht, 1993, p. 121.
[18] T.M. Abdel-Fattah, K.J. Balkus, Jr., G. Davies, S.A. Jansen and J. Leiton, submitted for publication.
[19] O.A. Tataev, S.A. Akhmedov and K.A. Akhmedova, Zhur. Analit. Chem., 24 (1969) 834.
[20] N.D. Chasteen, R.J. DeKoch, B.R. Rogers and M.W. Hanna, J. Am. Chem. Soc., 95 (1973) 4.
[21] Powder Diffraction File, Sets 21 to 22, International Center for Diffraction Data, Swarthmore, PA, 1980, pp. 54, 180, 673, 959.
[22] R.A. Nyquist and R.O. Kagel, Editors, Infrared Spectra of Inorganic Compounds, Academic, New York, 1971, pp. 84, 85.
[23] V.F. Kiselev and O.V. Krylov, Editors, Adsorption and Catalysis on Transition Metals and Their Oxides, Springer, Berlin, 1989, pp. 80–84, 240–242, 258.
[24] H. Matsumoto and S. Tanabe, J. Phys. Chem., 94 (1990) 4207 and references therein.
[25] G. Davies, M.A. El-Sayed and A. El-Toukhy, Chem. Soc. Rev., 21 (1992) 101.
[26] A. Abu-Raqabah, G. Davies, M.A. El-Sayed, A. El-Toukhy and M. Henary, Inorg. Chem., 28 (1989) 1156.
[27] S. Kawi, J.-R. Chang and B.C. Gates, J. Am. Chem. Soc., 115 (1993) 4830.
[28] G.G. Jernigan and G.A. Somerjai, J. Catal., 147 (1994) 567 and references therein.